Performance Analysis of an OWC Device Integrated within a Porous Breakwater

Rebecca Grennell [#1], Damon Howe [#2], Jean-Roch Nader [#3], Gregor Macfarlane[#4]

[#] *National Centre for Maritime Engineering & Hydrodynamics, Australian Maritime College, University of Tasmania Locked Bag 1395, Launceston, Tasmania 7250, Australia*

[1]beckygrennell@gmail.com

[2] damon.howe@utas.edu.au

[3] JeanRoch.Nader@utas.edu.au

[4]gregorm@amc.edu.au

The oscillating water column (OWC) wave energy converter is arguably the most heavily researched ocean renewable energy concept currently in development. Many variations of the concept have been proposed and explored, of which the bent duct type OWC has presented itself as one of the most effective concepts for absorbing ocean wave energy.

The integration of wave energy converters within maritime structures presents a number of advantages from an economic perspective, where it has been found that costs associated with construction, maintenance and grid connection can attribute as little as 3% toward the total cost of a traditional vertical caisson type breakwater [1]. Previous studies into the concept of breakwater integrated oscillating water column devices has focused on vertical caisson type breakwaters, or a generic rubble mound type breakwater, however little research has been conducted into the effect of breakwater reflectivity on the performance of the integrated OWC devices.

The experimental investigation was conducted in the Australian Maritime College's Model Test Basin facility, where a breakwater with controllable porosity was configured within an experimental set up with the aim of investigating the performance of an OWC device integrated within a porous breakwater.

The results indicate that an increase in breakwater reflection, along with a solid fitting increases device performance without major changes to the overall response curve of the device, with the greatest performance correlating to integration within a fully reflective breakwater.

***Keywords*— Oscillating Water Column, Wave Energy Converter, Porous Breakwater, Hydrodynamic Experimentation**

I. INTRODUCTION

As the global political and environmental climates change, so too does global investment in energy production. Interest in ocean renewable energy devices is growing with this global shift due to their applicability worldwide, availability of wave statistics, and greater energy density than other renewable sources [2]. Breakwaters are generally utilised for environmental protection purposes through the dissipation of waves in order to protect coastlines and ports, while an OWC WEC allows conversion of incident wave energy to electrical power. The incorporation of OWC devices within breakwaters can also reduce installation and maintenance costs, as well as provide easy access for ongoing operation and maintenance throughout the work life of the device [3]. This combination has the potential to make the concept of OWC devices more economical through shared structure costs. This paper investigates the response of an OWC device within a structure resembling a porous breakwater through hydrodynamic experimentation.

Tsinker [4] explains how a breakwater's primary objective is to provide calm waters for ship navigation, as they transform incident waves into reflected and transmitted waves. They can be constructed of rock rubble, engineered block rubble, concrete slabs, or a combination of these with a geometry that is sloped, vertical, floating, piled, or pneumatic. As breakwater design is highly variable, their ability to transform incident waves into reflected and transmitted waves also varies. Currently, accurate estimates of the reflective properties of a breakwater are generally obtained experimentally. However, it is known that wave reflection increases when the seaward slope angle increases, or the slope roughness or breakwater porosity decreases [5]. When designing a breakwater, it is recommended that a physical scale model of the design be tested, however, if wave reflection is all that is required then simple vertical wave screens can be used. Multiple wave screen designs have been tested for their reflective coefficient, which is simply the amplitude ratio of the reflected wave with respect to the incident wave.

The hydrodynamics of a wave screen comprising of horizontal slats was investigated in [6]. A theoretical model was derived and validated by using experimentally obtained results, which correlated well with those produced numerically. The results show that the reflection coefficient remains relatively constant and only slightly increasing with increasing incident wave frequency, and increases with increasing incident wave height. As expected, the reflection coefficient increases with decreasing porosity as there is more material to reflect the waves. A similar horizontally slotted breakwater was theoretically and experimentally tested in [7], who also found that the reflection coefficient increased with increasing wave frequency. A vertically slotted barrier was theoretically investigated in [8] with results that correlate with [6] and [7].

Many reviews and reports on the potential contribution of ocean energy within the global energy market have been transcribed in the last decade, from which the predominant issue being the lack of mature technologies [9-13]. Energy extraction from ocean waves is discussed in [14] with the primary finding being that a shore based OWC device would be a recommended choice of wave energy converter due to

reduced construction, grid connection and maintenance costs. If the coastline is of a concave form, the capture width of an OWC device will increase, as the waves will be channelled towards it. Correct choice of air chamber length with respect to incidence wave characteristics will also increase the capture width.

An OWC device at the tip of a breakwater was numerically studied according to [15]. The results showed that an isolated cylindrical OWC device has an absorption efficiency independent of the wave incidence angle. A cylindrical OWC device at the tip of a thin breakwater can theoretically achieve this independence. However, the required thinness of the breakwater for this to be achievable is not realistic and the geometry of the OWC device may diminish the independence of the incident wave angle.

Further study was completed for a numerical OWC device along a coast according to [16], with modelling that can be assumed as similar to an OWC device within a breakwater. The results showed that the absorption efficiency is now dependant on the wave incidence angle as is wave diffraction. The results also show that the capture width doubled, resulting from the induced wave reflection from the coast/breakwater.

A fully nonlinear numerical study of a shore-based OWC device was undertaken in [17] which utilised a PTO system with linear damping characteristics. The results obtained regarding linear incident waves concluded that increases to the seaward wall draft and thickness, and subsequent increase in the submerged chord length results in an increase in the resonance period of the OWC device, however reduces the capture efficiency. Similarly, it was also established that the optimal damping coefficient varied with regards to changes in draft and resonance period of the device.

Howe and Nader [18] conducted numerical and experimental tests on an isolated OWC device and an OWC device within a fully reflective wall. The results show that an OWC device within a fully reflective wall will have a higher energy absorption capacity than that of an isolated OWC device. In order to obtain comparable results, this paper adopts similar procedures to that of Howe and Nader.

This paper investigates physical model experimentation into the effect that breakwater porosity, and the subsequent reflectivity characteristics have on the performance of the breakwater integrated OWC device when subjected to monochromatic wave trains. A specially designed model scale breakwater was constructed, which allowed porosity and reflectivity characteristics to be experimentally varied and evaluated. This was achieved through use of sets of independently translatable breakwater panels, slats and bricks, allowing for the geometry of the breakwater to alter its porosity and reflection. The specifications of the breakwater design are discussed in Chapter III, and the reflection coefficients of the breakwater configurations were obtained using the three probe method proposed by Mansard and Funke [19].

II. THEORY

A. General

The hydrodynamic experimentation conducted considers a thin-walled bent duct OWC device integrated within a reflective breakwater structure, facing the incoming incident wave propagation. The surface piercing device operates in a constant water depth *h*. The previously used rectangular cross-sectioned device has an inlet width *D*, and an inlet height *W*, and a thickness *t*, with an internal chord length defined by the geometric components s_1, s_2, s_3 and s_4 (cf. Fig. 1 in [18]).

B. Breakwater Reflection

Currently, there are many potential methods for differentiating incident and reflected wave spectra during hydrodynamic experimentation. A review of the development in wave reflection estimations by Varghase et al. presents many different methodologies that have been developed since the 1970's [20]. This hydrodynamic experimentation of wave energy converter technology utilises the wave reflection estimation method derived by Mansard and Funke [19]. This method employs an array of three wave probes configured in front of the reflective structure that are spaced to predetermined distances as governed by the incident wavelength, as to adhere with the specifications outlined by Mansard and Funke.

C. OWC Performance

The methodology for quantifying absorption performance adheres to that previously utilised for hydrodynamic experimentation of this OWC device, as outlined in [18, 21, 22]. This includes the evaluation of the pneumatic damping coefficient of the PTO simulant, the volume flux of air through the PTO and its associated uncertainties, and the mean hydrodynamic power absorption. The device performance is quantified in terms of non-dimensional capture width, $\tilde{L}_{pc}$, as defined in Equation (1), which equates to the amount of energy absorbed by the device proportional to the incident wave energy of crest width correlating to the inlet width of the device.

$$\tilde{L}_{pc} = \frac{P_h}{P_I} \tag{1}$$

III. METHODOLOGY

A. Experimental Setup

1) Testing Facilities: The experimental investigation was conducted in the Australian Maritime Colleges shallow water wave basin, which is capable of producing regular and irregular wave spectra. The basin is 35 m long by 12 m wide with a mulit-element piston-type wave generator occupying one end of the basin, and a damping beach housed at the opposite. Its operational water depths are up to and including 1 m. A water depth of 600 mm with a wave height of 20 mm was used for this report to adhere to the hydrodynamic investigations conducted in [18, 21, 22]. The Model Test Basin specifications for this investigation are presented in Table I.

TABLE I
MODEL TEST BASIN SPECIFICATIONS

Item	Value	Dimension
Length	35.00	m
Width	12.00	m
Water Depth	00.60	m
Wave Height	00.02	m

2) Breakwater Model: The breakwater comprises of two size variations of horizontal wooden slats. The larger panels were 1200 mm in length, while the smaller panels were 600 mm in length, both having a thickness of 12 mm. The breakwater dimensions are presented in Table II.

TABLE II
BREAKWATER DIMENSIONS

Item	Value	Dimensions
Total Breakwater Length	4.500	m
Breakwater Height	0.900	m
Breakwater Thickness	0.012	m
Horizontal Slat Width	0.015	m
Horizontal Gap Width	0.025	m

The design of the model breakwater structure allowed for manual manipulation of horizontal slats, which were able to translate vertically. Once the desired level of vertical translation was achieved, the slotted panels were secured into place using a perpendicularly orientated nut and bolt mechanism operating within prefabricated guide rails through the panels.

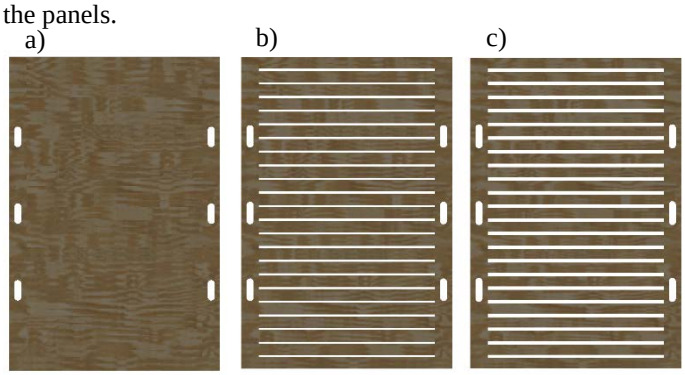

Fig. 1. Three variations of breakwater structural composition to represent a) zero porosity b) 0.15 porosity and c) 0.25 porosity

Utilising these design mechanisms, the breakwater model was able to operate within a porosity range of zero, correlating to a fully reflective breakwater, through to a porosity value of 0.25. The investigation considered both of these porosity values in the evaluation of device performance, along with an intermediate porosity value of 0.15 to provide a data set that would present the performance of the OWC device across three different porosity and reflectivity characteristics to determine any discernible trends that were evident. The three variations in panel structure that governed breakwater porosity are illustrated in Fig. 1.

3) OWC Model: The breakwater integrated OWC model-scale configuration comprises of an OWC device integrated at the centre of a porous breakwater structure as illustrated in Fig. 2. The OWC device is the rectangular model used in [18, 21, 22] having an inlet width of 0.3 m that remains constant throughout the structures geometry. The method for integrating the OWC device within the breakwater structure also utilised two variations in fitting parameters. Both the solid fitting and open fitting, illustrated in Fig. 3 and Fig. 4 respectively, were investigated to establish how the immediate area around the OWC device would affect the performance of the OWC device whilst integrated within a breakwater structure.

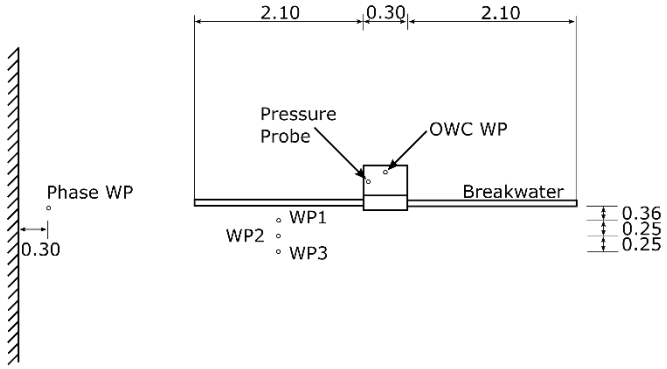

Fig. 2. Birds-eye schematic of the experimental apparatus labelled with relevant instrumentation and dimensions (not to scale, dimensions in mm).

Fig. 3. Solid wall fitting simulation for model scale OWC device integrated within porous breakwater.

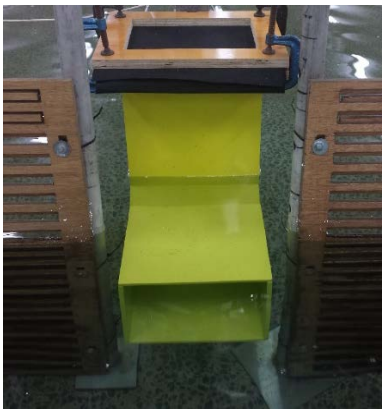

Fig. 4. OWC model integrated in the porous breakwater with no solid fitting.

4) Experimental Regime: With the OWC device installed, a resistive-type wave probe and pressure probe were configured

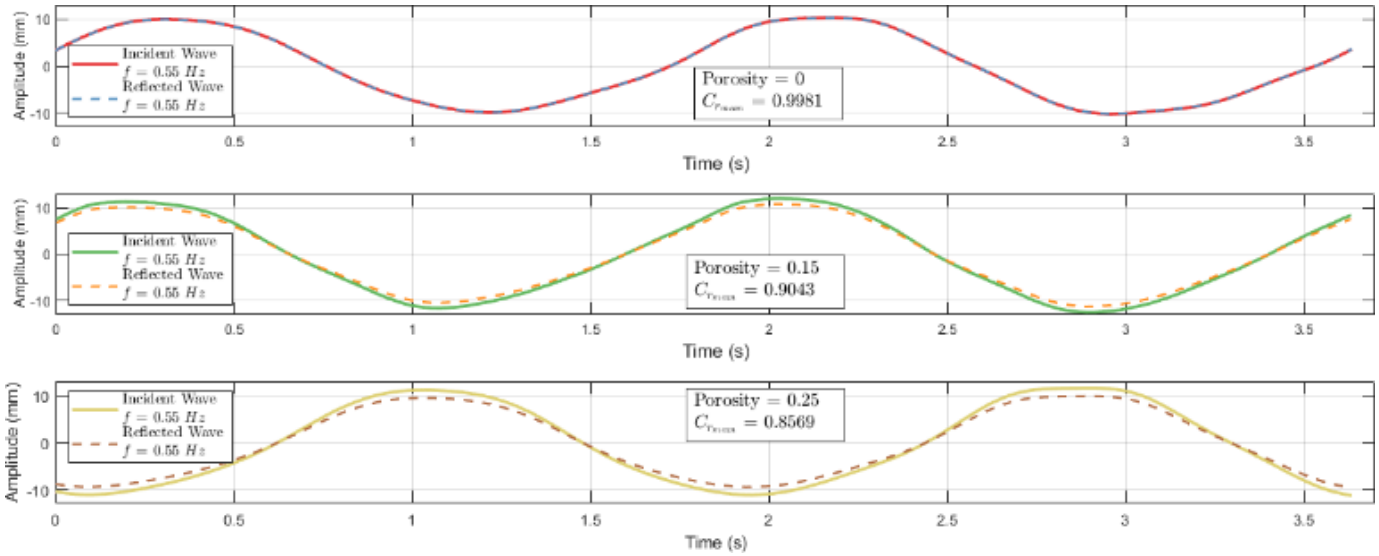

Fig. 5. Incident and reflected wave profiles across two wave periods for the a) 0 porosity b) 0.15 porosity and c) 0.25 porosity breakwater configurations

within the vertical chamber of the OWC device to record free surface elevation and dynamic chamber pressure respectively. Incident waves having constant height of 20 mm propagated towards the model with a frequency bandwidth of 0.5 Hz to 1.2 Hz. Reflectivity characteristics of the porous breakwater variations were recorded using three probes, WP1, WP2, and WP3, located forward of the breakwater parallel to wave direction of the incident wave train.

B. Data Processing

1) Phase Averaging: The experimental investigation focused specifically on regular waveforms of constant wave height and varying frequency in the evaluation of the OWC device performance. The sinusoidal nature of the subsequent data recorded allowed the phase-averaging post processing technique to be utilised for performance evaluation. With reference to previous investigations into this breakwater integrated OWC device [18, 21, 22], the technique was utilised to evaluating the values for incident wave height, η_0, and dynamic pressure amplitude, A_p, both of which are directly associated to the non-dimensional capture width of the device (cf. [18]). An experimental uncertainty analysis conducted on this OWC device determined that the phase averaging technique returns amplitude data that presents a standard deviation of approximately 2 % as percentage of the maximum amplitude when compared to 10 repeat runs [22]. Subsequently, the phase averaging post processing technique was found to both presented realistic and accurate results for sinusoidal data, whilst also reducing the time and resources necessary for regular wave tests.

2) Reflection Coefficients: A program was devised to evaluate the separation of reflected and incident wave spectra based on the methodology presented in [19]. Of particular importance regarding the evaluation of reflectivity characteristics was to ensure the data analysed was obtained from the reflected region of the measured data (cf. Fig. 9 in [18]). This allowed for the evaluation of the breakwaters reflection coefficient for variations in porosity and incident wave frequency, from which the mean results are presented in Section IV.

IV. Results

A. Reflection Characteristics

As the porosity of the model-scale breakwater was varied during the experimental test regime, so to was the respective reflectivity characteristics of the structure. Using the method previously established by Mansard and Funke [19], the experimental wave data for each individual run was separated into its incident and reflective components as presented in Fig. 5. This allowed the reflection coefficient to be derived for each experimental combination, from which the average reflection coefficient was established for each porosity variation as presented in Table III.

TABLE III
Cr_{MEAN} FOR BREAKWATER POROSITY VARIATIONS

Breakwater Porosity	**Mean Reflection Coefficient Cr_{mean}**
Porosity = 0	0.9981
Porosity = 0.15	0.9043
Porosity = 0.25	0.8569
Porosity = 1	0

As presented in Fig. 5, the relationship between breakwater porosity and reflection coefficient followed a trend indicating that as breakwater porosity increases, the reflectivity characteristics of the structure decrease. The three porosity variations of 0, 0.15 and 0.25 had average reflection coefficients, Cr_{mean}, of 0.9981, 0.9043 and 0.8569 respectively as presented in Table III. As can be noted from Fig. 5, the variation of reflection coefficient across the three porosity configurations is approximately 0.15, as such to fully investigate the relationship between breakwater porosity,

reflectivity characteristics and device performance, future experimental work incorporating configurations of greater porosity and subsequent less reflection should be considered.

B. Pneumatic Damping Characteristics

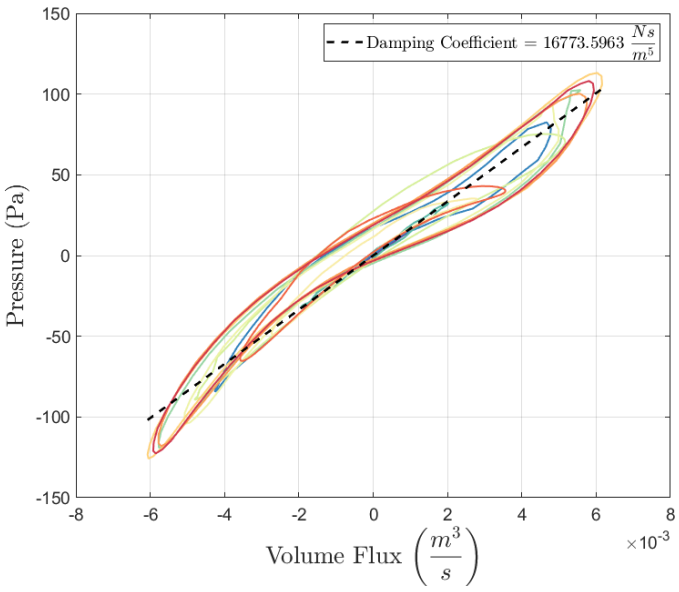

Fig. 6. Pneumatic damping relationship between pressure and volume flux for 0 porosity breakwater configuration.

Evaluation of the pneumatic damping characteristics of the PTO simulant using the previously established methodologies yielded the relationship illustrated in Fig. 6. Fig. 6 presents the damping relationship for the reflection coefficient variation correlating to a Cr_{mean} of 0.9043. As illustrated, the approximately linear relationship between internal dynamic pressure, p_c, and volume flux, Q, is maintained across the experimentally investigated porosity variations, with minimal deviation in the magnitudes of the pneumatic damping coefficient, δ, across the test cases, remaining within a range of ± 2.66 % between maximum and minimum magnitudes.

The approximately linear relationships presented as part of this investigation remains consistent with previously studies of the PTO simulant and OWC device in that the derived pneumatic damping coefficient is frequency independent, and is subsequently applied uniformly across all experimental incident wave frequencies to aid in evaluating device performance [18, 21, 22].

Fig. 6 also displays noticeable particulars regarding hysteresis and the effects of air compressibility in small-scale WEC technology. Firstly, all damping relationships displayed a discernible magnitude of hysteresis similar to that found in Fig. 6, which can be attributed to one of two factors. The first factor is associated with sealing issues associated with the connection of the PTO simulant to the outlet of the device, which results in pressure leak particularly noticeable on the upstroke of the internal water volume oscillation. Secondly, the integration of the PTO fabric mesh into the experimental apparatus requires a taut configuration of the fabric across the outlet of the device, as this reduces the hogging and sagging of the material when under the influence of the bi-directional airflow. It was observable during the experimental testing that the material displayed hogging/sagging of some degree, introducing uncertainties into the evaluation of the approximately linear damping relationship and will need further investigation for specific quantification of the effect on the presented results.

Regarding the effect of air compressibility, and with reference to other works produced by the authors [23], the relationships presented in Fig. 6 display no discernible phase shift between the pressure and volume flux that is typically associated with the effects of air compressibility. This lack of phase shift can be visualised in as the maximum and minimum values for volume flux correlate accordingly with the respective values for pressure. As presented in [23], the effect of air compressibility on the damping characteristics and subsequently the performance of this OWC device is not apparent until the air chamber volume approaches 0.5 cubic metres. To incorporate these effects into the current study, further investigation is required to establish the relationship between air chamber volume and air compressibility in small-scale WEC tank testing.

C. OWC Power Output

The OWC device performance was derived using the methods presented in [18], which utilise the pneumatic damping coefficient, δ, and the amplitude of dynamic air pressure. Fig. 7 illustrates the performance results of the OWC device for several breakwater porosities and integrational configurations tested. The results display the non-dimensional capture width, $\tilde{L}_{pc}$, with respect to the experimental incident wave frequency.

The integration of an OWC device within a maritime structure such as a breakwater has found to significantly increase the performance characteristics of the device at model scale as in [18]. The increase in performance can be attributed in part to the reflective nature of a solid vertical wall breakwater, which in theory should reflect 100% of the incident waves, subsequently having a reflection coefficient of 1. Device integration within such a structure impacts both the magnitude of energy absorption, and the bandwidth of incident wave frequencies in which the device will effectively operate. As presented in [18], the peak performance of a breakwater integrated device in comparison to its complementary isolated device can be almost twice the magnitude at the natural resonance frequency of the device.

Contrarily, the performance of an isolated device, fundamentally possessing a reflection coefficient of 0, operates effectively within a much reduced bandwidth and offers lower magnitudes of energy absorption. The isolated device investigated in [18] presented a particularly interesting characteristic in its overall response curve which indicated at an incident wave frequency of approximately 1 Hz a node appeared in the performance of the device. This particular characteristic was present in two geometric variations of the device, and appears an evident trait of the particular model being investigated.

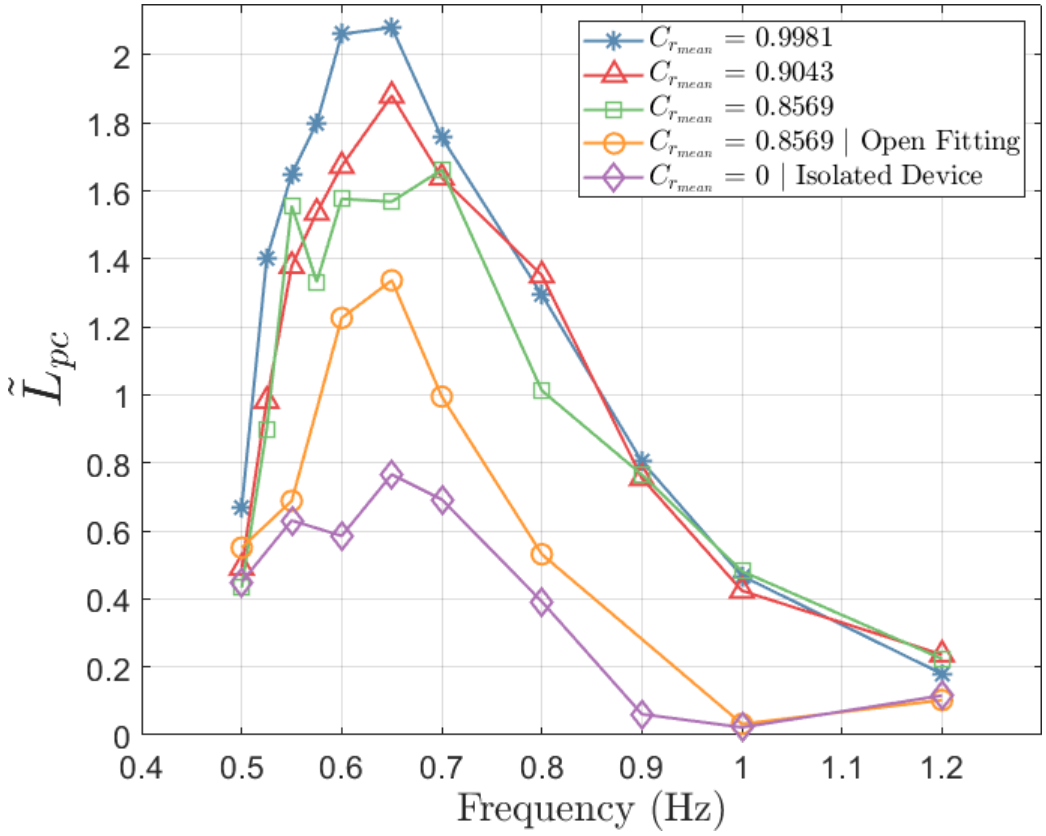

Fig. 7 Non-dimensional capture width, $\tilde{L}_{pc}$, versus incident wave frequency for the three breakwater porosity variations.

The performance results obtained for the OWC device throughout the experimental investigation are illustrated in Fig. 7. The performance of the OWC device is quantified as the non-dimensional capture width, $\tilde{L}_{pc}$, as defined by Equation (1), and is plotted with respect to the incident wave frequencies along the x-axis. The device integration variations (characterised by the contrasting coloured lines) include four different reflectivity conditions and two alterations in fitting arrangements. It should be noted that results presented in Fig. 7 excluding the isolated and open fitting configurations (characterised by the diamond and circular data points respectively), are devices operating within a solid fitted configurations.

Firstly analysing the results for variations in the reflectivity characteristics of the breakwater structure, it can be observed that as the reflection coefficient of the integrated structure tends towards one, the performance characteristics of the OWC device increase. This most evident at and around the natural resonance frequency of the device, where the values of performance are approximately 2.1 and 1.6 for reflection coefficients of 0.9981 and 0.8569 respectively. This trend correlates well with the results presented in [18], where the solid incorporation of an OWC device within a reflective structure significant increases the absorption performance of the device, again evident in Fig. 7.

Investigating the fitting configuration of the OWC device within the reflective structure, Fig. 7 illustrates the effect that the immediate area around the device can have on the absorption potential. Firstly focusing on the low incident wave frequencies corresponding to larger wavelengths, the reflective wall into which the device is integrated plays a more predominant role in the device performance, characterised by the sharp rise in performance at frequencies below resonance. As the device operates close to the resonant frequency, it is evident that as wavelength decreases the distance between the reflective structures and the area immediately around the breakwater becomes more important, represented by a significant reduction in the magnitude of performance. The solid fitting configuration operates far more effectively at resonance as opposed to the open fitting, which can be attributed to the reflective properties of the solid fill in the area immediately around the device.

Moving away from resonance into higher frequency, shorter wavelength incident waves, the open fitted device performance trends more towards the response curve of the isolated device, while the solid fitting follows the increase bandwidth performance of the other breakwater integrated structures. This further validates the importance of the spacing between reflective structures and the area immediately around the breakwater, as the shorter wavelengths interactions have more of a detrimental effect on performance of the open fitting configuration. The trend towards the isolated response curve of the open fitted configuration is most evident at 1 Hz, where the performance node is adopted by the breakwater integrated device. Adversely, the solid fitted device trend towards a consistent value relative to the other reflective structures as the reflectivity characteristics cease to have significant effect on the performance of the device in shorter wavelengths.

The significant disparity in the results obtained for devices integrated within identical reflective structures with different fitting parameters has major implications regarding the design and integration of OWC devices within multi-use maritime structures. The area immediately surrounding the device, in culmination with the spacing between reflective structures surrounding the device can reduce both the magnitude and bandwidth of absorption performance as wavelength decreases. The solid fitting configuration presents a more realistic representation of what would be expected for full scale integration, and provides the benefit of increase bandwidth and magnitude in higher frequencies regardless of the reflectivity characteristics of the surrounding structure in model scale, when compared to the isolated or open fitting configurations. The reflectivity characteristics of the structure have a significant effect on the performance of the device, particularly in larger wavelengths, however as wavelength decreases, the performance converges and is more reliant upon the fitting configuration.

It should be noted that the capture width and subsequent energy absorption potential for this device in its various configurations is sub-optimal. Previous works by Howe et al. found that the inlet lip extrusion of an OWC device from a breakwater structure negatively impacts the performance characteristics of the device, subsequently the optimal configuration is no extrusion which was not employed during this experimental investigation [21]. Similarly, the damping for each configuration was not optimised, therefore in practice under optimal damping conditions the device could potentially absorb a greater amount of incident wave energy. In reference to the performance characteristics of this device, Orphin et al. conducted an experimental uncertainty analysis on this particular OWC model, from which the results for $\tilde{L}_{pc}$ can vary up to approximately ± 30 % (cf. [22]). These variations can be attributed to both the hysteresis associated with pressure leaks illustrated in Fig. 6, along with the assumed linearity of the pneumatic damping relationship associated with the fabric mesh PTO simulant.

Concerning full-scale implementation of a breakwater-integrated concept, a device incorporated within a fully reflective vertical breakwater, having a solid fitting configuration would likely absorb the most incident wave energy based on the results obtained from these experiments. It is recommended that further investigation to explore breakwater structures with varying reflection coefficients, including more realistic structures like rubble mound or sloping breakwaters be conducted to further analyse the relationship between device performance, fitting characteristics and reflection coefficients. Similarly, further large-scale experiments should be conducted before any pre-commercial product is considered as the scaling effects of wave energy converter technologies is yet to be fully understood.

V. Conclusions

This hydrodynamic experimental investigation successfully integrated an OWC device within a porous breakwater model with the ability to vary porosity through simple geometry translations. The investigation showed that the reflection coefficient of the model breakwater can be controlled through this variation in porosity.

The performance of the OWC device was found to be dependent upon two important configurational factors, the breakwater reflectivity characteristics, and the integrated fitting of the device. A trend was established indicating as breakwater reflectivity increased, OWC device performance increased, most notably in the low frequencies and around resonance before converging to similar performance values regardless of porosity as wave length decreased. Similarly, the integration of the OWC device regarding a solid or open fitting highlighted the importance of the area immediately surrounding the device, and the separation between the reflective structures in which the device is integrated.

In longer wavelengths, the reflectivity characteristics of the structure influence device performance significantly, yet as the device operates at resonance and the moves towards shorter wavelengths, the open fitting and subsequent separation between structures has an evident detrimental effect on device performance.

Future works should include but not be limited to increasing breakwater porosity to establish whether the trend is consistent across a broader sample size. Similarly, investigation into a more realistic breakwater structure with porous features such as a rubble mound breakwater should be considered and hydrodynamically tested when an OWC device is integrated within the structure to compare the reflectivity characteristics to that of the vertical wall type structure investigated in this publication, along with further study into the fitting parameter and the effect it has in more realistic breakwater structures.

Acknowledgements

The authors would like to acknowledge Mr. Tim Lilianthal for assistance in the design and configuration of the model breakwater, as well as Mr. Kirk Meyer and Mr. Adam Rolls for their technical assistance during testing.

References

[1] Naty, S., A. Viviano, and E. Foti. "Feaseability study of a wec integrated in the port of giardini naxos, italy," in *Proceedings of 35th Conference on Coastal Engineering*. 2017. Antalya, Turkey.

[2] Blaabjerg, F. and D.M. Ionel, "Renewable Energy Devices and Systems – State-of-the-Art Technology, Research and Development, Challenges and Future Trends," *Electric Power Components and Systems*, vol. 43, pp.1319-1328, 2015.

[3] Falcão, A.F. and J.C. Henriques, "Oscillating-water-column wave energy converters and air turbines: A review," *Renewable Energy*, vol. 85, pp.1391-1424, 2016.

[4] Tsinker, G.P., *Port engineering: planning, construction, maintenance, and security*. John Wiley & Sons 2004.

[5] Dickson, W., T. Herbers, and E. Thornton, "Wave reflection from breakwater," *Journal of waterway, port, coastal, and ocean engineering*, vol. 121, pp.262-268, 1995.

[6] Bennett, G., P. Mciver, and J. Smallman, "A mathematical model of a slotted wavescreen breakwater," *Coastal Engineering*, vol. 18, pp.231-249, 1992.

[7] Rageh, O. and A. Koraim, "Hydraulic performance of vertical walls with horizontal slots used as breakwater," *Coastal Engineering*, vol. 57, pp.745-756, 2010.

[8] Suh, K.-D., C.-H. Ji, and B.H. Kim, "Closed-form solutions for wave reflection and transmission by vertical slotted barrier," *Coastal Engineering*, vol. 58, pp.1089-1096, 2011.

[9] Esteban, M., A. Gasparatos, and C.N. Doll, *Recent Developments in Ocean Energy and Offshore Wind: Financial Challenges and Environmental Misconceptions*, in *Sustainability Through Innovation in Product Life Cycle Design*. 2017, Springer. p. 735-746.

[10] Ipcc, *Special Report on Renewable Energy Sources and Climate Change Mitigation*, ed. C.U. Press. United Kingdom and New York, NY, USA: Cambridge University Press 2011.

[11] Krewitt, W., K. Nienhaus, C. Kleßmann, C. Capone, E. Stricker, W. Graus, M. Hoogwijk, N. Supersberger, U. Von Winterfeld, and S. Samadi, *Role and Potential of Renewable Energy and Energy Efficiency for Global Energy Supply*, in *Climate change*. 2009, Federal Environment Agency: Dessau-Roßlau, Germany.

[12] Lewis, A., S. Estefen, J. Huckerby, W. Musial, T. Pontes, and J. Torres-Martinez, *Ocean Energy. In IPCC Special Report on Renewable Energy Sources and Climate Change Mitigation [O. Edenhofer, R. Pichs-Madruga, Y. Sokona, K. Seyboth, P. Matschoss, S. Kadner, T. Zwickel, P. Eickemeier, G. Hansen, S. Schlömer, C. von Stechow (eds)]*, Cambridge University Press, Editor. 2011: Cambridge, United Kingdom and New York, NY, USA.

[13] Ren21, *Renewables 2016 Global Status Report*. Paris: REN21 Secretariat 2016.

[14] Mei, C.C., "Hydrodynamic principles of wave power extraction," *Phil. Trans. R. Soc. A*, vol. 370, pp.208-234, 2012.

[15] Martins-Rivas, H. and C.C. Mei, "Wave power extraction from an oscillating water column at the tip of a breakwater," *Journal of Fluid Mechanics*, vol. 626, pp.395-414, 2009.

[16] Martins-Rivas, H. and C.C. Mei, "Wave power extraction from an oscillating water column along a straight coast," *Ocean Engineering*, vol. 36, pp.426-433, 2009.

[17] Luo, Y., J.-R. Nader, P. Cooper, and S.-P. Zhu, "Nonlinear 2D analysis of the efficiency of fixed oscillating water column wave energy converters," *Renewable Energy*, vol. 64, pp.255-265, 2014.

[18] Howe, D. and J.-R. Nader, "OWC WEC integrated within a breakwater versus isolated: Experimental and numerical theoretical study," *International Journal of Marine Energy*, vol. 20, pp.165-182, 2017.

[19] Mansard, E.P. and E. Funke, *The measurement of incident and reflected spectra using a least squares method*, in *Coastal Engineering 1980*. 1980. p. 154-172.

[20] Varghese, R., K. Shirlal, B. Hari, and S. Mohanan, "Review of Developments in Estimation of Wave Reflection from Coastal Structures," *IOSR Journal of Mechanical and Civil Engineering*, vol. 30-32, 2016.

[21] Howe, D., J.-R. Nader, J. Orphin, and G. Macfarlane. "The Effect of Lip Extrusion on Performance of a Breakwater Integrated Bent Duct OWC WEC," in *European Wave and Tidal Energy Conference*. 2017. Cork, Ireland.

[22] Orphin, J., J.R. Nader, I. Penesis, and D. Howe. "Experimental Uncertainty Analysis of an OWC Wave Energy Converter," in *Proceedings of 12th European Wave and Tidal Energy Conference*. 2017. Cork, Ireland.

[23] Howe, D., J.-R. Nader, and G. Macfarlane. "Experimental Analysis into the Effects of Air Compressibility in OWC Model Testing," in *Proceedings of the 4th Asian Wave and Tidal Energy Conference*. 2018. Taipei, Taiwan. *(Submitted Pending Acceptance)*